Since January 2020 Elsevier has created a COVID-19 resource centre with free information in English and Mandarin on the novel coronavirus COVID-19. The COVID-19 resource centre is hosted on Elsevier Connect, the company's public news and information website.

Chaos, Solitons and Fractals 139 (2020) 110296

Contents lists available at ScienceDirect

Chaos, Solitons and Fractals

Nonlinear Science, and Nonequilibrium and Complex Phenomena

journal homepage: www.elsevier.com/locate/chaos

Simulation of coronavirus disease 2019 (COVID-19) scenarios with possibility of reinfection

Egor Malkov[a,b]

[a] Department of Economics, University of Minnesota, 1925 Fourth Street South, Minneapolis, MN 55455, USA
[b] Federal Reserve Bank of Minneapolis, 90 Hennepin Ave, Minneapolis, MN 55401, USA

ARTICLE INFO

Article history:
Received 6 June 2020
Revised 4 September 2020
Accepted 12 September 2020
Available online 18 September 2020

Keywords:
SEIRS model
Epidemiological dynamics
COVID-19
Reinfection
Mitigation

ABSTRACT

Epidemiological models of COVID-19 transmission assume that recovered individuals have a fully protected immunity. To date, there is no definite answer about whether people who recover from COVID-19 can be reinfected with the severe acute respiratory syndrome coronavirus 2 (SARS-CoV-2). In the absence of a clear answer about the risk of reinfection, it is instructive to consider the possible scenarios. To study the epidemiological dynamics with the possibility of reinfection, I use a Susceptible-Exposed-Infectious-Resistant-Susceptible model with the time-varying transmission rate. I consider three different ways of modeling reinfection. The crucial feature of this study is that I explore both the difference between the reinfection and no-reinfection scenarios and how the mitigation measures affect this difference. The principal results are the following. First, the dynamics of the reinfection and no-reinfection scenarios are indistinguishable before the infection peak. Second, the mitigation measures delay not only the infection peak, but also the moment when the difference between the reinfection and no-reinfection scenarios becomes prominent. These results are robust to various modeling assumptions.

1. Introduction

The rapid spread of coronavirus disease 2019 (COVID-19) creates significant challenges for economies and healthcare systems of many countries around the world. The situation evolves extremely quickly and, to date, there is a high degree of uncertainty about the future outcomes of the pandemic. As of September 1, 2020, there have been 25.9 million confirmed cases globally, including about 860 thousand deaths, see [28].

One of the crucial questions that still has no definite answer is whether people who recover from COVID-19 can be reinfected with the severe acute respiratory syndrome coronavirus 2 (SARS-CoV-2). The case reports are scarce — there are a few of them about positive testing after recovering from COVID-19 in China, Japan, and South Korea — and it is not clear whether these patients are truly reinfected or not. Shi et al. [24] discuss the immune responses induced by COVID-19. Another study, Bao et al. [4], using the sample of four rhesus macaques, conclude that the primary SARS-CoV-2 infection could protect from subsequent reinfections. In turn, An et al. [1], show that 38 out of 262 patients, i.e. 14.5 percent, recovered from COVID-19, tested positive for SARS-CoV-2, using polymerase chain reaction (PCR) tests, after being discharged from the hospital in Shenzhen. Those patients did not show obviously clinical symptoms and disease progression upon readmission. A recent study by To et al. [25] shows the results of the whole genome sequencing that was performed directly on respiratory specimens collected during two episodes of COVID-19 in a patient. Epidemiological, clinical, serological, and genomic analyses confirmed that the patient had reinfection instead of persistent viral shedding from the first infection. Their paper suggests that SARS-CoV-2 may continue to circulate among the human populations despite herd immunity due to natural infection or vaccination.

In the absence of a clear answer about the risk of reinfection with the new coronavirus, it is instructive to be aware of the possible scenarios. This study aims at providing the attempt in this direction. I use a Susceptible-Exposed-Infectious-Resistant-Susceptible (SEIRS) model that differs from a standard SEIR model, considered in Hethcote [11] and Chowell et al. [8], and, in application to COVID-19, Kucharski et al. [14], Lin et al. [18], Prem et al. [20], and Wang et al. [27], among others, with an additional assumption that recovered individuals can become susceptible to infection again. In methodologically related papers, Reynolds et al. [22] and Etbaigha et al. [9] study the reinfection of swines with influenza A virus (IAV). The simulations considered in this paper are by no means the definitive quantitative forecasts. Instead, the purpose is to show the patterns of the disease dynamics if people

E-mail address: malko017@umn.edu

https://doi.org/10.1016/j.chaos.2020.110296
0960-0779/

can be reinfected with the new coronavirus. In fact, the risk of reinfection would definitely affect the scope and duration of policies that are currently in place.

I consider three different ways of modeling reinfection. I begin with the model where individuals have constant immunity waning rate and study the effects of the mitigation policies captured by the changes in the transmission rate and hence the reproduction number. The basic reproduction number, R_0, is a crucial parameter for evaluation the spread of the infection and the effects of mitigation measures. Existing estimates for COVID-19 suggest that R_0 is between 2 and 6. Using the data from Wuhan, China, Wu et al. [29] estimate R_0 to be 2.68 (95% confidence interval (CI): 2.47–2.86). Using the data from mainland China, Zhao et al. [30] conclude that the mean estimate of R_0 ranges from 2.24 (95% CI: 1.96–2.55) to 3.58 (95% CI: 2.89–4.39). Using the data for Italy, Remuzzi and Remuzzi [21] propose R_0 to be in the range 2.76–3.25. Using the data for Japan, Kuniya [15] estimates R_0 to be 2.6 (95% CI: 2.4–2.8). Fauci et al. [10] propose R_0 to be 2.2. Sanche et al. [23] obtain a higher median estimate, $R_0 = 5.7$ (95% CI: 3.8–8.9). Beyond that, Korolev [13] shows that estimates of R_0 are highly sensitive to the values of epidemiologic parameters. In the simulations, I consider the range of values of the basic reproduction number.

Crucially, in each model experiment I consider not only how different are the reinfection and no-reinfection scenarios, but also how the mitigation measures affect this difference. To check the robustness of my findings about the role of the mitigation measures with and without reinfection, I turn to the alternative modeling assumptions about reinfection. First, I assume that individuals, once being reinfected, have a milder form of the disease. Second, instead of a constant immunity waning rate, I assume that the individuals that are resistant at some date (those who were infected in the past) become susceptible again. The conceptual framework that I use can be easily incorporated into more complex models in future studies.

2. Model

Consider a SEIRS model with constant population N normalized to one. Each period of time, the population consists of four classes: susceptible (S), exposed (E), infected (I), and resistant (recovered) (R):

$$S(t) + E(t) + I(t) + R(t) = N, \qquad \forall t \geq 0 \tag{1}$$

Since $N = 1$, variables S, E, I, and R correspond to the fractions of the population. I assume that recovered individuals can become susceptible to infection again at rate ω. The compartmental model is formulated by the following set of ordinary differential equations:

$$\frac{dS(t)}{dt} = -\beta(t)\frac{S(t)}{N}I(t) + \omega R(t) \tag{2}$$

$$\frac{dE(t)}{dt} = \beta(t)\frac{S(t)}{N}I(t) - \sigma E(t) \tag{3}$$

$$\frac{dI(t)}{dt} = \sigma E(t) - \gamma I(t) \tag{4}$$

$$\frac{dR(t)}{dt} = \gamma I(t) - \omega R(t) \tag{5}$$

The transmission rate, $\beta(t)$, accounts for the rate at which infected individuals interact with others and transmit the disease and is given by

$$\beta(t) = \gamma \tilde{R}(t) \tag{6}$$

where $\tilde{R}(t)$ is the time-varying reproduction number. Absent mitigation measures, $\tilde{R}$ corresponds to the basic reproduction number, R_0. To simplify notation, here and thereafter I omit explicit dependence of $\tilde{R}$ on time whenever it does not cause confusion. The transmission rate, $\beta(t)$, captures the impact of all mitigation measures such as quarantine, travel restrictions, or social distancing. To study scenarios under different mitigation policies, I adapt a flexible functional form for the time-varying reproduction number. Following [3], I parameterize $\tilde{R}(t)$ as follows:

$$\tilde{R}_1(t) = \exp(-\eta_1 t)\tilde{R}_1(0) + (1 - \exp(-\eta_1 t))R_1^* \tag{7}$$

$$\tilde{R}_2(t) = \exp(-\eta_2 t)\tilde{R}_2(0) + (1 - \exp(-\eta_2 t))R_2^* \tag{8}$$

$$\tilde{R}(t) = \frac{1}{2}\left(\tilde{R}_1(t) + \tilde{R}_2(t)\right) \tag{9}$$

where $\tilde{R}_1(0)$ and $\tilde{R}_2(0)$ (R_1^* and R_2^*) are the initial (long-run) values for $\tilde{R}_1$ and $\tilde{R}_2$. Parameter η_1 determines the rate at which $\tilde{R}_1$ converges to R_1^*. In turn, parameter η_2 governs the rate at which $\tilde{R}_2$ converges to R_2^*. By appropriately choosing the parameter values, I can capture different scenarios of the mitigation policies. In particular, in the simulations in Section 3, I vary the speed of imposing the mitigation measures and also consider the scenario when extremely severe mitigation measures at the beginning of the pandemic are followed by their gradual relaxation. From (7)–(9), the dynamics of $\tilde{R}_1$, $\tilde{R}_2$, and $\tilde{R}$ is described by the following equations:

$$\frac{d\tilde{R}_1(t)}{dt} = -\eta_1(\tilde{R}_1(t) - R_1^*) \tag{10}$$

$$\frac{d\tilde{R}_2(t)}{dt} = -\eta_2(\tilde{R}_2(t) - R_2^*) \tag{11}$$

$$\frac{d\tilde{R}(t)}{dt} = -\frac{1}{2}\eta_1\left(\tilde{R}_1(t) - R_1^*\right) - \frac{1}{2}\eta_2\left(\tilde{R}_2(t) - R_2^*\right) \tag{12}$$

Parameters (σ, γ, ω) represent the characteristics of COVID-19 and assumed to be constant. For parameters σ and γ, I take the estimates from the literature. The parameter σ stands for the mean incubation period of the disease, and its estimates vary from 1/5.2 to 1/3, see [18] and [27]. Following [16] and [27], I adopt a mean latent period of 5.2 days (infection rate, $\sigma = 1/5.2$). Next, I adopt a mean infectious period of 18 days (recovery rate, $\gamma = 1/18$) in line with [7] and [27]. Parameter ω, the immunity waning rate, is of the main interest for this paper, and since, to date, there are no credible estimates of it, I consider the range of different values, $\omega \in \{0, 1/365, 1/183, 1/120, 1/60\}$. To et al. [25] show that the second episode of asymptomatic infection occurred 142 days after the first symptomatic episode in an apparently immunocompetent patient. This period is consistent with considered range of ω. The case $\omega = 0$ corresponds to no reinfection. The value of ω is driven by immunity waning after the infection or the rate of virus mutation. Next, the initial values for actively infected and exposed population are taken for the United States and set to $I(0) = 1/1000$, i.e. 0.1 percent of the population, and $E(0) = 43.75 \times I(0)$ respectively. I use March 16–17, 2020 as the initial date (March 17, 2020 was a day at which the last U.S. state reported its first case, see [19]). I take $I(0) = 1/1000$ from [5]. Official data reports around 4500 cases in the United States on March 16, and they assume that this represents 1.5 percent of all cases. This rate of underreporting is derived by Hortaçsu et al. [12] for March 9, 2020. $E(0) = 43.75 \times I(0)$ corresponds to the estimates for the United States by Peirlinck et al. [19].

Throughout the simulations, I fully acknowledge that only a fraction of the model-generated cases are reported in reality. Li et al. [17] study the critical importance of undocumented COVID-19 cases for understanding the overall prevalence and pandemic potential of this disease. Lin et al. [18] emphasize that the reporting rate is time-varying.

3. Model simulations

In this section, I use the assumptions about the time paths for $\tilde{R}$ from [3]. This allows me to clearly compare the outcomes under reinfection with his conclusions from the simulations without reinfection. In the first model experiment, I assume that $\tilde{R}$ is fixed over time. This reflects the scenarios when mitigation efforts do not change over time.

In the first model experiment, I consider a range of values of the basic reproduction number $\tilde{R} = R_0 \in \{1.6, 1.8, 2.0, 2.2, 2.5, 2.8, 3.0\}$. The upper bound of this range captures the estimates from the literature discussed in Section 1. Lower values of R_0 correspond to lower levels of the disease transmission. The mitigation measures — quarantine, travel restrictions, or social distancing — can reduce the basic reproduction number. Anderson et al. [2] provide a thorough discussion of this question. Critically, in my simulations, I vary both ω and R_0. By comparing the simulated series under different values of ω and R_0, I follow two goals. First, given R_0, I compare the outcomes of the reinfection and no-reinfection scenarios. Second, given ω, I demonstrate the effects of the mitigation measures (expressed through the lower values of R_0) under the reinfection and no-reinfection scenarios.

Fig. 1 shows the time paths for the simulated fraction of the actively infected population with (solid lines) and without (dashed lines) reinfection under different values of R_0. This model experiment implies that lower R_0 leads to delaying the infection peak both with and without reinfection. Second, under the reinfection scenario, the size of the peak is greater than without reinfection. The difference in the peak values is decreasing in R_0. Third, with reinfection, the fraction of the actively infected population exhibits asymmetric dynamics around the peak. Crucially, before the peak, the time paths with and without reinfection are indistinguishable. However, after the peak, the reinfection series is unambiguously above the no-reinfection series. Therefore, by reducing the transmission rate with the mitigation measures, we delay the infection peak, and hence delay the moment when the difference between the reinfection and no-reinfection scenarios becomes sizeable. Finally, notice that, with reinfection, there can be multiple-wave disease outbreaks. In a related study, [6] discuss the role of homologous reinfection in driving multiple-wave influenza outbreaks. Next, Fig. 1e contains the phase diagram where I plot the fraction of the susceptible population against the fraction of the actively infected population. The solution of the model under both reinfection and no-reinfection scenarios starts in the bottom right corner where $I(0)$ is close to zero and $S(0)$ is close to one. This phase diagram also illustrates that before the peak two scenarios — with and without reinfection — are almost indistinguishable.

In the second model experiment, I assume that $\tilde{R}$ gradually decreases at different speed. To capture the scenarious under different speed of implementation, following [3], I set $\tilde{R}_1(0) = \tilde{R}_2(0) = 3$, $R_1^* = R_2^* = 1.6$, and vary parameters η_1 and η_2 with $\eta_1 = \eta_2 \equiv \eta$. There are five scenarios: very fast ($\eta = 1/5$), fast ($\eta = 1/10$), moderate ($\eta = 1/20$), slow ($\eta = 1/50$), and very slow ($\eta = 1/100$). Higher values of η govern higher rate of convergence of $\tilde{R}$ to the long-run value of 1.6. Fig. 2 shows the time paths for $\tilde{R}$ and the simulated fraction of the actively infected population with (solid lines) and without (dashed lines) reinfection. This model experiment implies that the speed of implementation affects the timing of the peak and its size. Faster implementation of mitigation measures leads to delaying the infection peak both with and without reinfection. Next, similarly to the simulation from Fig. 1, under the reinfection scenario, the fraction of the actively infected population exhibits asymmetric dynamics around the peak. Relative to the no-reinfection scenario, reinfection affects the epidemic duration, the size of the infection peak, and the timing of the infection peak. Furthermore, to provide additional evidence to the dynamics of the solution, in Fig. 2b I show the phase diagram where plot the fraction of the susceptible population against the fraction of the actively infected population.

In the third model experiment, I assume that $\tilde{R}$ significantly drops at the beginning, as a result of extremely severe mitigation measures, and then gradually goes up, as the mitigation measures are relaxed. Following [3], I set $\tilde{R}_1(0) = 10$, $\tilde{R}_2(0) = -4$, $R_1^* = -10$, $R_2^* = 4$, $\eta_1 = 1/35$, and $\eta_2 = 1/100$. Given the initial and long-run values of the reproduction number and $\eta_1 > \eta_2$, $\tilde{R}_1(t)$ is rapidly decreasing function while $\tilde{R}_2(t)$ is slowly increasing function. As a result, the time path for $\tilde{R}(t)$ has a U-shaped form, see Fig. 3a. The other two panels of Fig. 3 show the simulated fraction of the actively infected population with and without reinfection. Under the temporary and extremely severe mitigation measures, in the first four months, as shown in Fig. 3b, the fraction of the actively infected population substantially goes down. Moreover, the dynamics is identical for the scenarios with and without the possibility of reinfection. Turning to the first 15 months of the pandemic, shown in Fig. 3c, we see that gradual relaxation that follows the initial extremely severe mitigation measures, leads to a subsequent peak. Therefore, relaxation of the mitigation measures, driven by the optimistic dynamics in the first months, eventually leads to the epidemic. Motivated by the observation that early mitigation measures delay the peak but not its size, because the population does not acquire herd immunity, Toda [26] studies the optimal mitigation policy. He shows that it is optimal to initiate the mitigation measures once the number of cases reaches some threshold fraction of the population.

4. Alternative reinfection assumptions

4.1. Milder disease after reinfection

I consider two alternative ways of modeling reinfection. First, I assume that individuals, once being reinfected, have a milder form of the disease. This is in line with [1] who discuss the clinical characteristics of the recovered COVID-19 patients with redetectable positive RNA test. When readmitted to the hospital, these patients showed no obvious clinical symptoms or disease progression. In the model, I assume that the individuals who become susceptible after being recovered, have lower transmission rate and higher recovery rate. At each point in time, the population, normalized to one, consists of seven classes: primary-susceptible (S_p), secondary-susceptible (S_s), primary-exposed (E_p), secondary-exposed (E_s), primary-infected (I_p), secondary-infected (I_s), and resistant (recovered) (R):

$$S_p(t) + S_s(t) + E_p(t) + E_s(t) + I_p(t) + I_s(t) + R(t) = N, \qquad \forall t \geq 0 \tag{13}$$

Individuals belong to S_p, E_p, or I_p if they were not infected before. Individuals belong to S_s, E_s, or I_s after being recovered. The compartmental model is formulated as follows:

$$\frac{dS_p(t)}{dt} = -(\beta_p I_p(t) + \beta_s I_s(t))\frac{S_p(t)}{N} \tag{14}$$

$$\frac{dS_s(t)}{dt} = -(\beta_p I_p(t) + \beta_s I_s(t))\frac{S_s(t)}{N} + \omega R(t) \tag{15}$$

$$\frac{dE_p(t)}{dt} = (\beta_p I_p(t) + \beta_s I_s(t))\frac{S_p(t)}{N} - \sigma_p E_p(t) \tag{16}$$

$$\frac{dE_s(t)}{dt} = (\beta_p I_p(t) + \beta_s I_s(t))\frac{S_s(t)}{N} - \sigma_s E_s(t) \tag{17}$$

$$\frac{dI_p(t)}{dt} = \sigma_p E_p(t) - \gamma_p I_p(t) \tag{18}$$

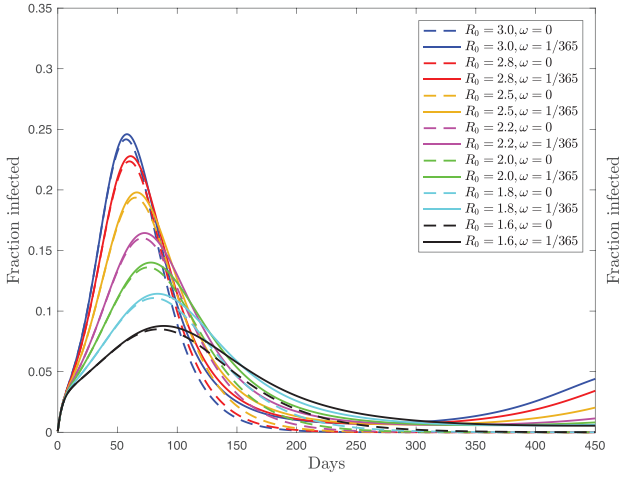

(a) Immunity waning rate $\omega = 1/365$.

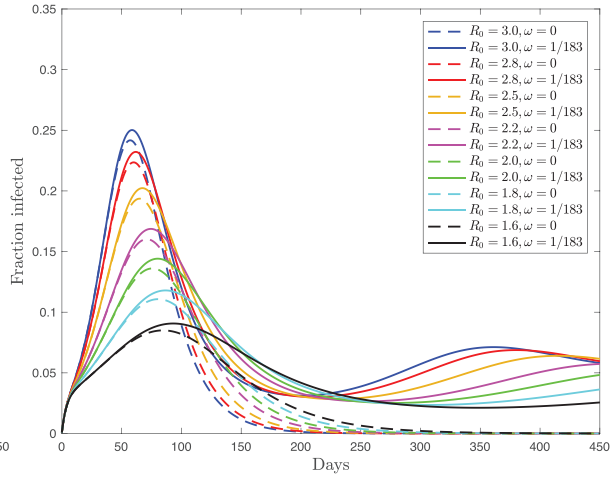

(b) Immunity waning rate $\omega = 1/183$.

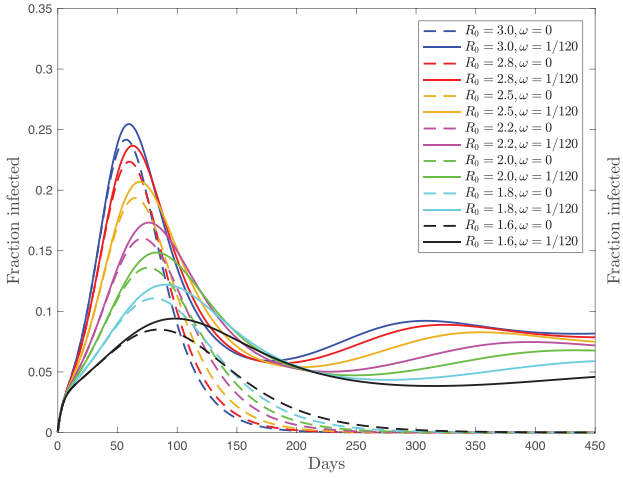

(c) Immunity waning rate $\omega = 1/120$.

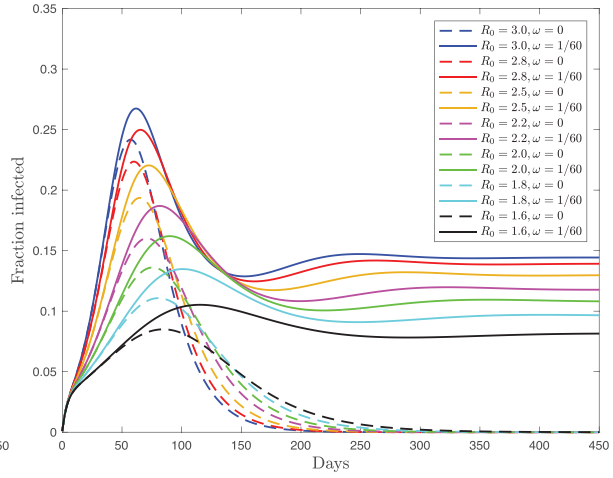

(d) Immunity waning rate $\omega = 1/60$.

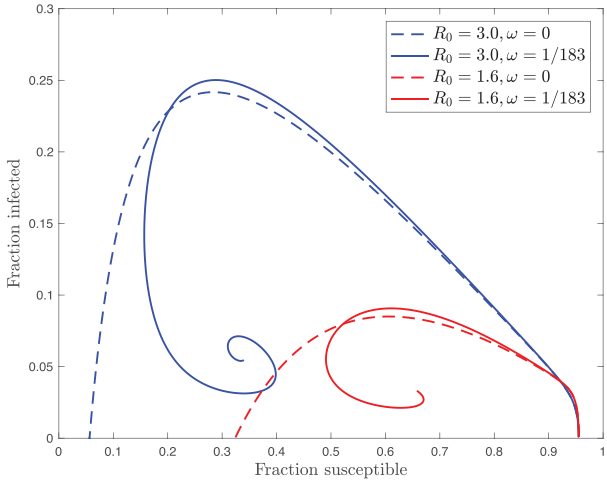

(e) S-I phase diagram, $\omega = 1/183$.

Fig. 1. Panels (a)–(d) show the fraction of the actively infected population over time under the reinfection (solid) and no-reinfection (dashed) scenarios and with different values of the basic reproduction number, R_0. Panels (a)–(d) differ in the size of the immunity waning ratio, ω. Panel (e) contains the phase diagram that shows the evolution of the fraction of the actively infected population against the fraction of the susceptible population with and without reinfection.

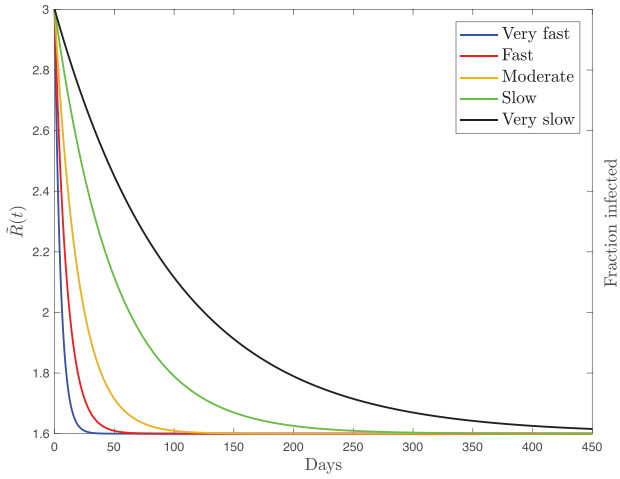

(a) Time-varying $\tilde{R}$.

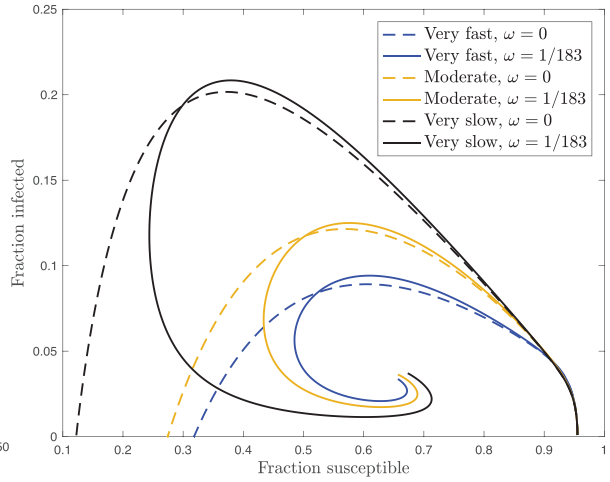

(b) S-I phase diagram, $\omega = 1/183$.

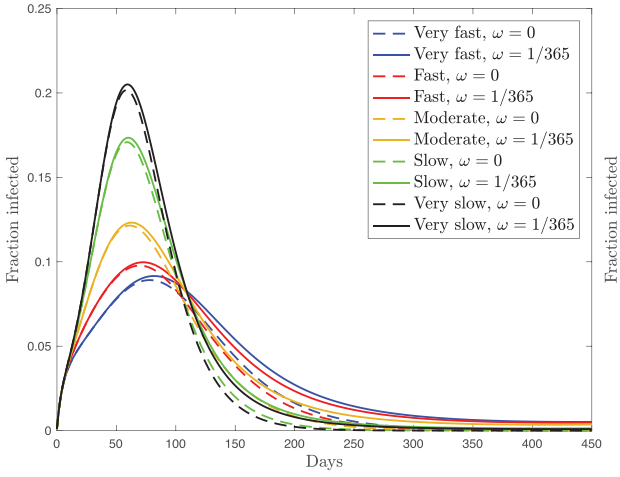

(c) Immunity waning rate $\omega = 1/365$.

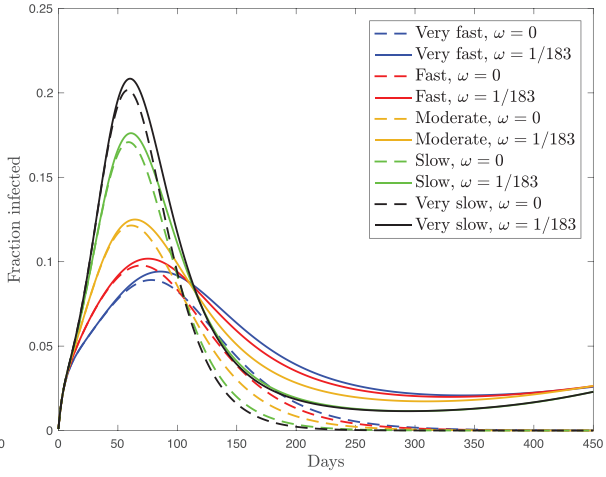

(d) Immunity waning rate $\omega = 1/183$.

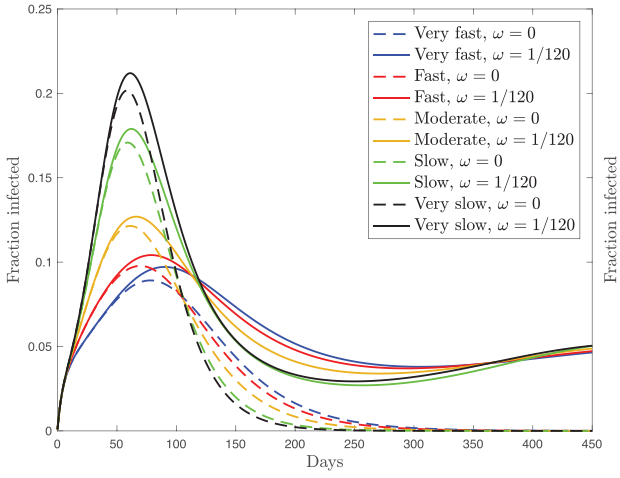

(e) Immunity waning rate $\omega = 1/120$.

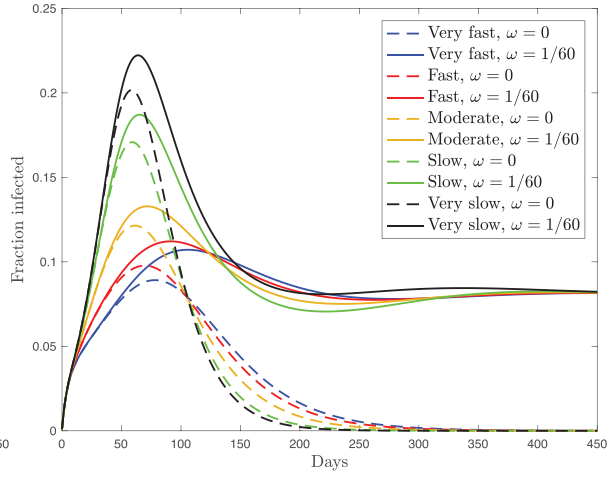

(f) Immunity waning rate $\omega = 1/60$.

Fig. 2. Panel (a) shows the time paths for the time-varying reproduction number, $\tilde{R}$. Panel (b) contains the phase diagram that shows the evolution of the fraction of the actively infected population against the fraction of the susceptible population with and without reinfection. Panels (c)–(e) show the fraction of the actively infected population over time under the reinfection (solid) and no-reinfection (dashed) scenarios and with different speed of the change in $\tilde{R}$. Panels (c)–(e) differ in the size of the immunity waning ratio, ω.

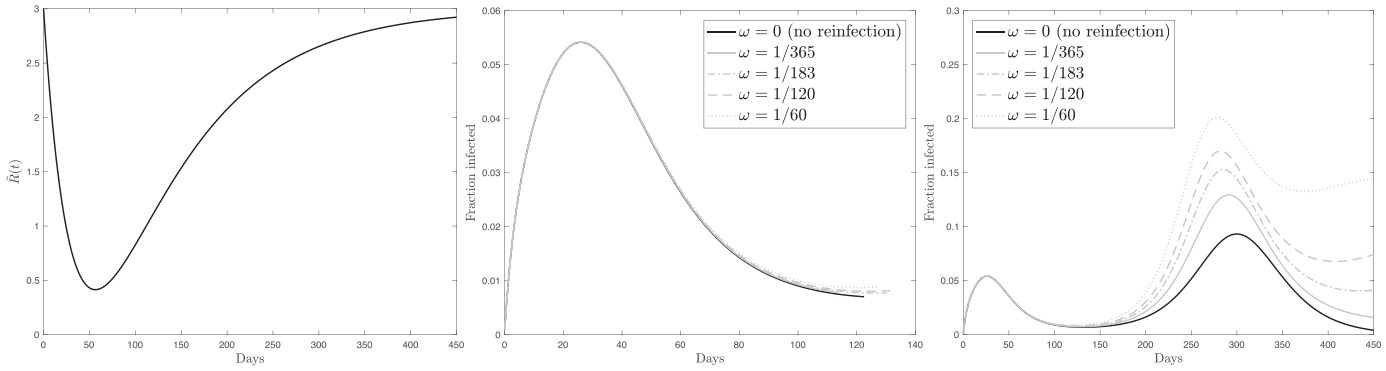

(a) Time-varying $\tilde{R}$. (b) Infected, first 4 months. (c) Infected, first 15 months.

Fig. 3. Panel (a) shows the time path for the time-varying reproduction number, $\tilde{R}$. Panel (b) shows the fraction of the actively infected population over time under the temporary and extremely severe mitigation measures in the first 4 months. Panel (c) shows the fraction of the actively infected population over time under the temporary and extremely severe mitigation measures in the first 15 months. In panels (b) and (c), black solid line ($\omega = 0$) corresponds to the no-reinfection scenario. The grey lines ($\omega > 0$) correspond to the reinfection scenarios. The lines coincide in panel (b).

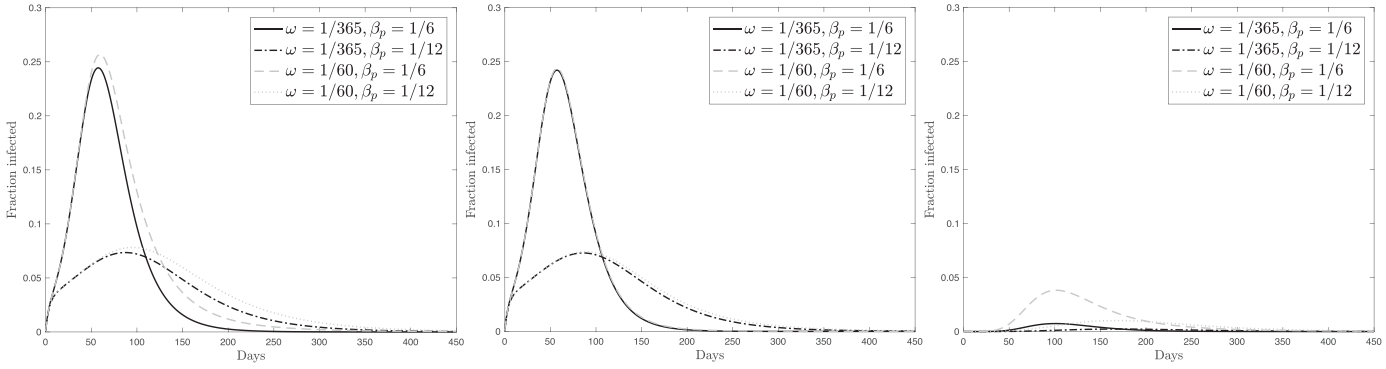

(a) Infected (total). (b) Primary-infected. (c) Secondary-infected.

Fig. 4. Panel (a) shows the fraction of the total (primary and secondary) actively infected population over time. Panel (b) shows the fraction of the actively primary-infected population over time. Panel (c) shows the fraction of the actively secondary-infected population over time. Panels (a)–(c) consider various combinations of the immunity waning rate, ω, and the primary-transmission rate, β_p.

$$\frac{dI_s(t)}{dt} = \sigma_s E_s(t) - \gamma_s I_s(t) \tag{19}$$

$$\frac{dR(t)}{dt} = \gamma_p I_p(t) + \gamma_s I_s(t) - \omega R(t) \tag{20}$$

Note that susceptible individuals, both those who have never been infected and those who have recovered and are currently susceptible again, become exposed after contacting with both primary- and secondary-infected individuals. In the absence of the parameter estimates for COVID-19, I assume that $\beta_s = \beta_p/2$, $\gamma_s = 2\gamma_p$, and $\sigma_s = \sigma_p$. Following the previous simulations, I set $\sigma_p = 1/5.2$ and $\gamma_p = 1/18$. The initial values are $I_p(0) = 1/1000$, $E_p(0) = 43.75 \times I_p(0)$, as in Section 2, and $S_s(0) = E_s(0) = I_s(0) = R(0) = 0$.

Fig. 4 shows the simulated time paths for the fraction of the actively infected population — total (primary and secondary), primary, and secondary. In these simulations, I consider several scenarios. They are characterized by four combinations of the immunity waning rate and primary-transmission rate, β_p. The immunity waning rate takes two values, $\omega = 1/365$ and $\omega = 1/60$. Thus, I use the lower and upper bounds of the range considered in the previous simulations. The primary-transmission rate also takes two values, $\beta_p = 1/6$ and $\beta_p = 1/12$. The case $\beta_p = 1/6$ corresponds to $R_0 = 3.0$ in the baseline SEIRS model from Section 2, while the case $\beta_p = 1/12$ corresponds to $R_0 = 1.5$. We can see from Fig. 4 that the dynamics of the total fraction of the actively infected population is almost entirely driven by the primary-infected people. There is a limited role of reinfection in the general epidemic dynamics.

4.2. One-time reinfection

Second, instead of a constant immunity waning rate, I assume that the individuals, that are resistant at date t^* (those who were infected in the past), become susceptible again. In particular, I consider a standard SEIR model, i.e. one described by Eqs. (1)–(5) with $\omega = 0$. Before date t^*, the dynamics of the model coincides with the no-reinfection case. At date t^*, resistant individuals join the pool of susceptible population. Formally this is described by $S(t^*) = S(t^* - dt) + R(t^* - dt)$ as $dt \to 0$. Therefore, at date t^* the fraction of resistant population goes down to zero, while the fraction of susceptible population discretely goes up. To illustrate the patterns that arise under this modeling approach of reinfection, I choose two time thresholds, $t^* = 120$ and $t^* = 30$.

Fig. 5 shows the time paths for the fraction of the actively infected population. For each scenario, I consider a range of the basic reproduction number values. First, my model simulations imply that if the infection peak occurs before t^*, as in Fig. 5a, then reinfection leads to a double peak. Second, if the infection peak occurs shortly after t^*, as in Fig. 5b, then reinfection results in a higher single peak. Notice that the simulated series are consistent with the conclusion from Section 3 that the mitigation measures (lower

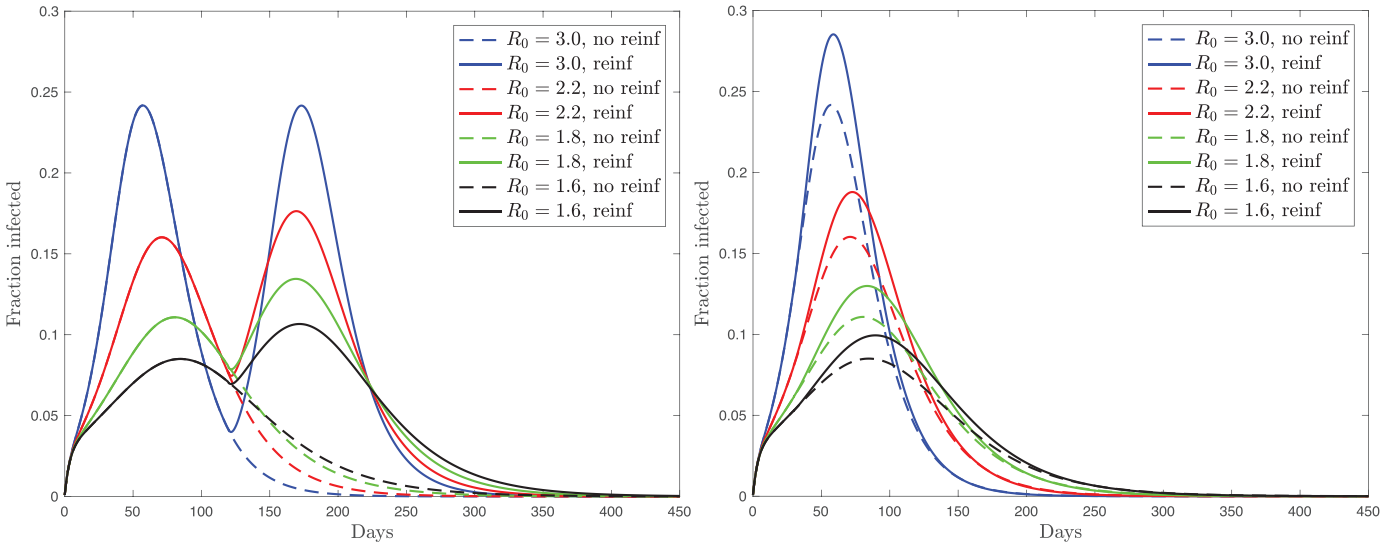

(a) Reinfection time $t^* = 120$. (b) Reinfection time $t^* = 30$.

Fig. 5. Fraction of the actively infected population over time under the reinfection (solid) and no-reinfection (dashed) scenarios and with different values of the basic reproduction number, R_0. Panels (a) and (b) differ in the time of reinfection.

R_0) delay not only the infection peak, but also the moment when the difference between the reinfection and no-reinfection scenarios becomes prominent.

5. Conclusion

To date, the immune response, including duration of immunity, to SARS-CoV-2 infection is not yet understood. Unless it is clearly known that patients with COVID-19 are unlikely to be reinfected, it is instructive to consider the possible scenarios. In this paper, I study how the possibility of reinfection shapes the epidemiological dynamics at the population level. To explore the difference in the dynamics of the disease under the reinfection and no-reinfection scenarios and, furthermore, the effects of the mitigation measures, I use a SEIRS model and consider three different ways of modeling reinfection. A key finding is that the mitigation measures delay not only the infection peak, but also the moment when the difference between the reinfection and no-reinfection scenarios becomes prominent. This result is robust to various modeling assumptions. The framework is simple and therefore can serve as a baseline for more complex models.

Funding

This research did not receive any specific grant from funding agencies in the public, commercial, or not-for-profit sectors.

Declaration of Competing Interest

The authors declare that they have no known competing financial interests or personal relationships that could have appeared to influence the work reported in this paper.

Acknowledgments

I thank the editor, Gabriel B. Mindlin, and two anonymous referees for their constructive comments, which helped me to improve the manuscript. I thank Polina Protasova, James Stock, and Alexis Akira Toda for useful comments and discussion. All remaining errors are mine. The views expressed herein are those of the author and not necessarily those of the Federal Reserve Bank of Minneapolis or the Federal Reserve System.

References

[1] An J., Liao X., Xiao T., Qian S., Yuan J., Ye H., et al. Clinical Characteristics of the Recovered COVID-19 Patients with Re-Detectable Positive RNA Test. medRxiv 20200326200442222020; 10.1101/2020.03.26.20044222
[2] Anderson RM, Heesterbeek H, Klinkenberg D, Hollingsworth TD. How will country-based mitigation measures influence the course of the COVID-19 epidemic? Lancet 2020;395(10228):931–4. doi:10.1016/S0140-6736(20)30567-5.
[3] Atkeson AG. What will be the economic impact of COVID-19 in the US? Rough estimates of disease scenarios. NBER working paper No 26867; 2020. doi:10.3386/w26867.
[4] Bao L., Deng W., Gao H., Xiao C., Liu J., Xue J., et al. Reinfection Could not Occur in SARS-CoV-2 Infected Rhesus Macaques. bioRxiv, 2020; 10.1101/2020.03.13.990226
[5] Berger DW, Huang C, Herkenhoff KF, Mongey S. Reopening in an SEIR model with testing and targeted quarantine. University of Chicago Unpublished Manuscript; 2020.
[6] Camacho A, Cazelles B. Does homologous reinfection drive multiple-wave influenza outbreaks? Accounting for immunodynamics in epidemiological models. Epidemics 2013;5(4):187–96. doi:10.1016/j.epidem.2013.09.003.
[7] Chen N, Zhou M, Dong X, Qu J, Gong F, Han Y, et al. Epidemiological and clinical characteristics of 99 cases of 2019 novel coronavirus pneumonia in Wuhan, China: adescriptive study. Lancet 2020;395(10223):507–13. doi:10.1016/S0140-6736(20)30211-7.
[8] Chowell G, Hengartner NW, Castillo-Chavez C, Fenimore PW, Hyman JM. The basic reproductive number of ebola and the effects of public health measures: the cases of congo and uganda. J Theor Biol 2004;229(1):119–26. doi:10.1016/j.jtbi.2004.03.006.
[9] Etbaigha F, Willms AR, Poljak Z. An SEIR model of influenza a virus infection and reinfection within a farrow-to-finish swine farm. PLoS One 2018;13(9). doi:10.1371/journal.pone.0202493.
[10] Fauci AS, Lane HC, Redfield RR. COVID-19 — navigating the uncharted. N Engl J Med 2020. doi:10.1056/NEJMe2002387.
[11] Hethcote HW. The mathematics of infectious diseases. SIAM Rev 2000;42(4):599–653. doi:10.1137/S0036144500371907.
[12] Hortaçsu A, Liu J, Schwieg T. Estimating the Fraction of Unreported Infections in Epidemics with a Known Epicenter: An Application to COVID-19. Tech. Rep.; 2020. doi:10.3386/w27028.
[13] Korolev I. Identification and estimation of the SEIRD epidemic model for COVID-19. J Econom 2020. doi:10.1016/j.jeconom.2020.07.038.
[14] Kucharski AJ, Russell TW, Diamond C, Liu Y, Edmunds J, Funk S, et al. Early dynamics of transmission and control of COVID-19: a mathematical modelling study. Lancet Infect Dis 2020. doi:10.1016/S1473-3099(20)30144-4.
[15] Kuniya T. Prediction of the epidemic peak of coronavirus disease in Japan, 2020. J Clin Med 2020;9(3):789–95. doi:10.3390/jcm9030789.
[16] Li Q, Guan X, Wu P, Wang X, Zhou L, Tong Y, et al. Early transmission dynamics in Wuhan, China, of novel coronavirus-infected pneumonia. N Engl J Med 2020. doi:10.1056/NEJMoa2001316.

[17] Li R, Pei S, Chen B, Song Y, Zhang T, Yang W, et al. Substantial undocumented infection facilitates the rapid dissemination of novel coronavirus (SARS-CoV2). Science 2020. doi:10.1126/science.abb3221.
[18] Lin Q, Zhao S, Gao D, Lou Y, Yang S, Musa SS, et al. A conceptual model for the coronavirus disease 2019 (COVID-19) outbreak in Wuhan, China with individual reaction and governmental action. Int J Infect Dis 2020:211–16. doi:10.1016/j.ijid.2020.02.058.
[19] Peirlinck M, Linka K, Costabal FS, Kuhl E. Outbreak dynamics of COVID-19 in China and the United States. Biomech Model Mechanobiol 2020:1–15. doi:10.1007/s10237-020-01332-5.
[20] Prem K, Liu Y, Russell TW, Kucharski AJ, Eggo RM, Davies N, et al. The effect of control strategies to reduce social mixing on outcomes of the COVID-19 epidemic in wuhan, china: a modelling study. Lancet Public Health 2020. doi:10.1016/S2468-2667(20)30073-6.
[21] Remuzzi A, Remuzzi G. COVID-19 and Italy: what next? Lancet 2020. doi:10.1016/S0140-6736(20)30627-9.
[22] Reynolds JJ, Torremorell M, Craft ME. Mathematical modeling of influenza a virus dynamics within swine farms and the effects of vaccination. PLoS One 2014;9(8). doi:10.1371/journal.pone.0106177.
[23] Sanche S, Lin Y, Xu C, Romero-Severson E, Hengartner N, Ke R. High contagiousness and rapid spread of severe acute respiratory syndrome coronavirus 2. Emerg Infect Dis 2020;26(7). doi:10.3201/eid2607.200282.
[24] Shi Y., Wang Y., Shao C., Huang J., Gan J., Huang X., et al. COVID-19 Infection: The Perspectives on Immune Responses. 2020. 10.1038/s41418-020-0530-3
[25] To KK-W, Hung IF-N, Ip JD, Chu AW-H, Chan W-M, Tam AR, et al. COVID-19 Re-infection by a phylogenetically distinct SARS-coronavirus-2 strain confirmed by whole genome sequencing. Clin Infect Dis 2020. doi:10.1093/cid/ciaa1275.
[26] Toda A.A.. Susceptible-infected-recovered (SIR) dynamics of COVID-19 and economic impact. arXiv:200311221 2020.
[27] Wang H, Wang Z, Dong Y, Chang R, Xu C, Yu X, et al. Phase-adjusted estimation of the number of coronavirus disease 2019 cases in Wuhan, China. Cell Discov 2020;6(1):1–8. doi:10.1038/s41421-020-0148-0.
[28] Worldometers. Coronavirus cases, 2020, (accessed September 2, 2020) https://www.worldometers.info/coronavirus/.
[29] Wu JT, Leung K, Leung GM. Nowcasting and forecasting the potential domestic and international spread of the 2019-nCoV outbreak originating in Wuhan, China: a modelling study. Lancet 2020;395(10225):689–97. doi:10.1016/S0140-6736(20)30260-9.
[30] Zhao S, Lin Q, Ran J, Musa SS, Yang G, Wang W, et al. Preliminary estimation of the basic reproduction number of novel coronavirus (2019-nCoV) in China, from 2019 to 2020: a data-driven analysis in the early phase of the outbreak. Int J Infect Dis 2020;92:214–17. doi:10.1016/j.ijid.2020.01.050.